Longitudinal Imaging of Liver Cancer Using MicroCT and Nanoparticle Contrast Agents in CRISPR/Cas9-Induced Liver Cancer Mouse Model

Sang Bu An[1], Kwangmo Yang, MD, PhD[2], Chang Won Kim, MD, PhD[3], Si Ho Choi, PhD[4], Eunji Kim[2] ⓘ, Sung Dae Kim[4], and Jae Soo Koh[5]

Abstract

Introduction: Micro-computed tomography with nanoparticle contrast agents may be a suitable tool for monitoring the time course of the development and progression of tumors. Here, we suggest a practical and convenient experimental method for generating and longitudinally imaging murine liver cancer models. **Methods:** Liver cancer was induced in 6 experimental mice by injecting clustered regularly interspaced short palindromic repeats/clustered regularly interspaced short palindromic repeats-associated protein 9 plasmids causing mutations in genes expressed by hepatocytes. Nanoparticle agents are captured by Kupffer cells and detected by micro-computed tomography, thereby enabling longitudinal imaging. A total of 9 mice were used for the experiment. Six mice were injected with both plasmids and contrast, 2 injected with contrast alone, and one not injected with either agent. Micro-computed tomography images were acquired every 2- up to 14-weeks after cancer induction. **Results:** Liver cancer was first detected by micro-computed tomography at 8 weeks. The mean value of hepatic parenchymal attenuation remained almost unchanged over time, although the standard deviation of attenuation, reflecting heterogeneous contrast enhancement of the hepatic parenchyma, increased slowly over time in all mice. Histopathologically, heterogeneous distribution and aggregation of Kupffer cells was more prominent in the experimental group than in the control group. Heterogeneous enhancement of hepatic parenchyma, which could cause image quality deterioration and image misinterpretation, was observed and could be due to variation in Kupffer cells distribution. **Conclusion:** Micro-computed tomography with nanoparticle contrast is useful in evaluating the induction and characteristics of liver cancer, determining appropriate size of liver cancer for testing, and confirming therapeutic response.

Keywords

microCT, longitudinal imaging, nanoparticle contrast agents, mouse model, liver cancer, CRISPR/Cas9

[1] Department of Radiology, Korea Institute of Radiological and Medical Sciences, Nowon-gu, Seoul, Korea
[2] Department of Radiation Oncology, Korea Institute of Radiological and Medical Sciences, Nowon-gu, Seoul, Korea
[3] Department of Radiology, School of Medicine and Biomedical Research Institute, Pusan National University, Pusan National University Hospital, Busan, Korea
[4] Research Center, Dongnam Institute of Radiological and Medical Sciences, Busan, Korea
[5] Department of Pathology, Korea Institute of Radiological and Medical Sciences, Nowon-gu, Seoul, Korea

Corresponding Authors:
Kwangmo Yang, MD, PhD, Department of Radiation Oncology, Korea Institute of Radiological and Medical Sciences 75, Nowon-ro, Nowon-gu, Seoul 01812, Korea.
Email: eskimykm@gmail.com

Chang Won Kim, MD, PhD, Department of Radiology, School of Medicine and Biomedical Research Institute, Pusan National University, Pusan National University Hospital 179, Gudeok-ro, Seo-gu, Busan 49241, Korea.
Email: radkim@nate.com

Si Ho Choi, PhD, Research Center, Dongnam Institute of Radiological and Medical Sciences, Jwadong-gil 40, Jangan-eup, Gijang-gun, Busan 46033, Korea.
Email: sihochoi@gmail.com

Introduction

Animal models of cancer with characteristics similar to human cancer patients enable precision individualized cancer treatment. Various cancers, including liver cancer, have many genetic variations that vary from patient to patient.[1] Previously, the animal used to model liver cancer had to be sacrificed to gauge treatment response; however, imaging techniques have now emerged that can confirm cancerous lesions without sacrificing experimental animals.[2-4] One such technique, microcomputed tomography (microCT) with contrast agents, is suitable for use in small animals, and allows rapid, real-time evaluation in small animal models. However, no study to date has used CT imaging to confirm changes in cancer lesions over a long time period after inducing cancer, such as by injecting specific gene variants.

In mice, the contrast agents utilized are excreted via the kidneys in approximately 5 s, thereby allowing little contrast enhancement effect. New contrast agents with long-term retention in blood vessels and soft tissues are needed.[5-7] Previous studies of small animal contrast agents have implemented microCT and different types of nanoparticle contrast agents to evaluate contrast intensity, duration, and toxicity over time.[2,8]

Exitron nano (Viscover ExiTron nano 12000; Miltenyi Biotec, Bergisch-Gladbach, Germany) is a type of nanoparticle contrast agent which is captured and retained by the reticuloendothelial system, including liver Kupffer cells, allowing contrast agents to remain in the parenchyma longer.[2] Once administered, this agent has a contrast enhancement effect superior to that of other contrast agents that act on hepatocytes and lasting for 6 months or more.[2,9] These particles have an average diameter of 110 nm and are stabilized with a polymer coating and can be safely administered.[2,10] The agent is made of alkaline earth metal with an atomic number higher than iodine, allowing use of a small amount of agent for strong contrast enhancement.[5]

There are various methods of generating liver cancer in animal models. In this study, we utilized the recently developed clustered regularly interspaced short palindromic repeats (CRISPR)/CRISPR-associated protein 9 (Cas9) technology and hydrodynamic injection to induce liver cancer in mice rapidly, simply, and dependably.[11-14] Hydrodynamic injection has been used successfully to induce cancer both in the liver and lungs in previous studies.[12,15] Additionally, successful induction of liver cancer with simultaneous inhibition of phosphatase and tensin homolog (*PTEN*) and *p53* genes using CRISPR/Cas9 injection has also been reported.[11,16]

We used microCT and nanoparticle contrast agents for longitudinal imaging to evaluate the efficiency of the liver cancer induction method, to assess characteristics of the induced liver cancer, to select the appropriate size of liver cancer lesion, to assess the effectiveness of treatment, and to confirm treatment response.[17]

Materials and Methods

### Induction of Liver Cancer (CRISPR/Cas9 Plasmids Injection)

For CRISPR/Cas9 constructs, we used the px459 V2.0 (Addgene #108292) vector transcribing sgRNA and transiently expressing wild-type SpCas9. Three sgRNAs (sgPten and sgRb1, and sgCtnnb) were sequentially inserted into a px459 V2.0 vector linearized by BbsI. The plasmid also contains homologous recombination template containing 4 alanine point mutations which abolish the phosphorylation of serine and threonine sites of β-catenin.[18] In brief, pX459 plasmid was digested with BbsI and ligated with annealed oligonucleotides for Ctnnb1 sgRNA. The homologous recombination template for Ctnnb1 was PCR amplified and inserted into the NotI site of px459 plasmids using In-Fusion HD cloning kit (TAKARA). px459 plasmids expressing sgRNA for Pten and Rb1 were generated separately. U6 promoter and sgRNA for Pten and Rb1 were PCR amplified and sequentially inserted into the plasmid containing sgRNA and homologous recombination template for Ctnnb1 mutations. All primers used for cloning are listed in Supplementary Table 1.

Six experimental mice (C57BL/6 8-week-old, T01-T06) were injected with CRISPR/Cas9 plasmids causing mutations in genes related to cancer and expressed in hepatocytes. After preparing 60 μg of the plasmids and diluting it in 2 mL saline, the solution was hydrodynamically injected through a lateral tail vein using a 31-gauge syringe in 5-7 s. Two control mice (C01 and C02) were not injected with CRISPR/Cas9 plasmids. Additionally, one normal mouse (N01) did not receive CRISPR/Cas9 plasmids or contrast agent and was used for reference comparison with other animals. All C57BL/6 mice were purchased from DooYeol Biotech. (Seoul, Korea) and were randomly selected. Group allocation of the mice was unblinded. Experiments using animals were approved by the Dongnam Institute of Radiological & Medical Sciences Institutional Animal Care and Use Committee.

Contrast Agent Injection and MicroCT Scanning

Contrast agent was administered 2 weeks after cancer induction. Imaging began 4 h after contrast media administration, given that enhancement is strongest 4-8 h after contrast administration.[2] Six experimental and 2 control mice were injected with 150 μL of the ExiTron nano 12000 contrast agent through the lateral tail vein using 31-gauge syringes. MicroCT (NFR Polaris-G90, NanoFocus Ray Co., Ltd., Jeonju, Korea) scans were obtained on the day of contrast agent administration and every 2 weeks up to 12-14 weeks after CRISPR/Cas9 plasmid injection.

Before microCT, animals were anesthetized by intraperitoneal injection of a 200-μL mixture of zolazepam, tiletamine (Zoletil 50®, 10 mg/kg, Virbac, Carros, France) and xylazine (Rompun®,10; Bayer, Leverkusen, Germany). MicroCT imaging was performed without tracheal intubation, continuous
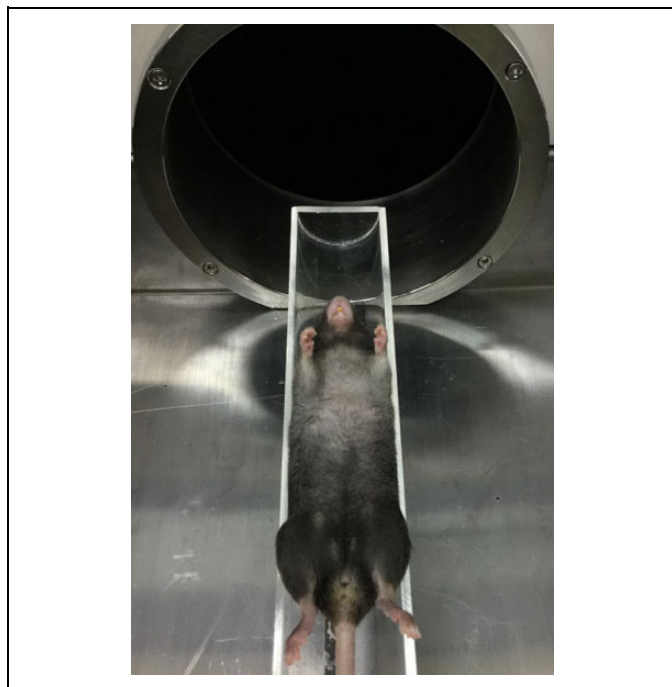
Figure 1. Anesthetized mouse lying on the scanning table before micro-computed tomography (microCT): good quality images could be obtained without any additional respiratory or cardiac gating device. The mouse did not present activity during scanning. After 6 microCT scans, loss and whitening of hair in the scanning target area on the mouse abdomen was observed.

inhalation anesthesia, or heart rate synchronization (Figure 1). To obtain a good quality image, the averaging technique built into microCT (a method of deriving an average image by repeating a scan several times) was used. The scan parameters were as follows: 80 kV, 75 µA; spot size, 8 mm; exposure time, 150 ms; scan angle, 360°; scan number, 420; image size, 512 × 512 pixels; magnification, × 4; average, 3; reconstruction algorithm: filtered Feldkamp back projection. A summary of the experiments is presented in Figure 2.

Image Analysis

Because ExiTron nano is a negative contrast agent, liver cancer appears as a hypoattenuated area. We evaluated the timing and size of the first visible liver cancer nodule and change in size and number of lesions during longitudinal imaging. We presented time-course imaging of one mouse (T03) as an example of longitudinal imaging. The T03 mouse demonstrated liver cancer at the earliest time point on microCT and was observed for 14 weeks.

To evaluate the change in overall contrast enhancement intensity and degree of heterogeneous contrast enhancement of the hepatic parenchyma, the mean value and standard deviation (SD) of CT attenuation were measured by applying the maximum region of interest (ROI) to the right liver lobe. The mean value is an indicator of contrast enhancement intensity, and the SD reflects the degree of heterogeneous contrast
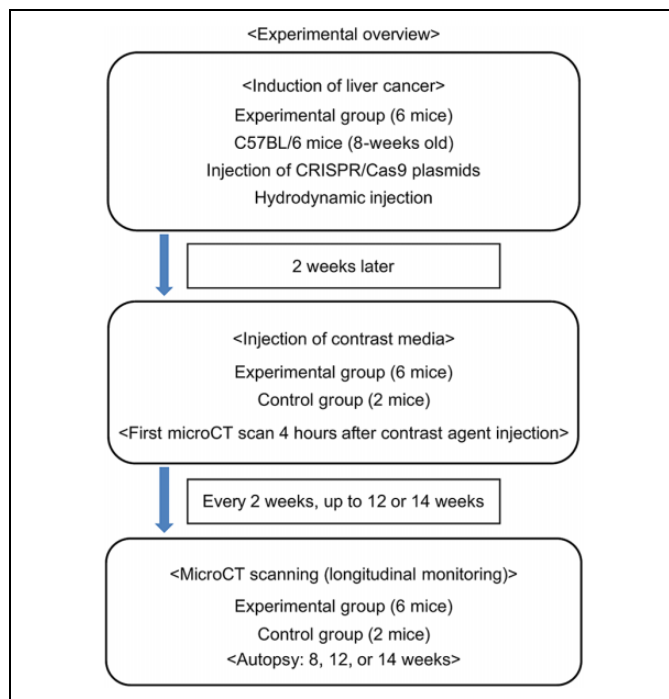
Figure 2. Experimental overview.

enhancement of the liver parenchyma. Considering the shape of the right lobe, the ROI was set as an ellipsoid with a minimum area of 30.00 mm^2 and was chosen to avoid errors in measurement of hepatic parenchymal attenuation, given the reduced overlap of blood vessels (portal and hepatic veins) among the various lobes of the liver. The cross-sections used for measurements were selected as sections where the branching vessels of the right portal and right hepatic veins were absent or minimally visible. Measurements were performed on 2 experimental mice (T02 and T03), which reflected the latest and earliest development of liver cancer, respectively, and that survived up to 14 weeks as both mice (C01 and C02) in the control group.

Comparison of Pathological and Image Results

Four mice were sacrificed at 12 weeks and another 4 at 14 weeks; their livers were harvested and subjected to pathological examination using hematoxylin and eosin staining. Hepatic cancer lesions were identified on histopathology and correlated with microCT imaging.

Results

Induction of Liver Cancer (CRISPR/Cas9 Plasmids Injection) and Contrast Agent Injection

To develop a mouse live cancer model, we chose 3 genes, Pten, Rb1, and Ctnnb1 that are known to be frequently mutated in liver cancer.[19] To generate somatic mutations for these genes, we delivered a plasmid DNA expressing Cas9 and single guide

RNAs (sgRNAs) for Pten, Rb1, and Ctnnb1 into the mouse liver through hydrodynamic injection.[11]

Infusion of CRISPR/Cas9 plasmids by hydrodynamic injection was successful in all 6 experimental mice. Two weeks post-injection, the appearance and activity of the mice were good until contrast agent injection. Contrast agent injection was attempted in all experimental and control mice. In all except for one experimental mouse (T01), the contrast agent was properly injected and the hepatic parenchyma was successfully enhanced. One experimental mouse (T04) died 8 weeks after liver cancer induction. The remaining mice survived without noticeable activity problems till experiment completion (weeks 12-14).

MicroCT Scanning

Mice were anesthetized before microCT imaging, and it was easy to maintain anesthesia with additional anesthetic agent (50% of the initial dose), even if this implied a longer waiting time before scanning. MicroCT images were taken every 2 weeks for each mouse, totaling 6 to 7 scans. Of note, varying degrees of hair loss and whitening of the abdominal imaging area were grossly observed in 5 surviving experimental mice and 2 control mice by experiment conclusion.

Summary of the Experiment Results

Liver cancer was first detected on microCT imaging 8 weeks after cancer induction. In the T03 mouse, the single nodule cancer that was initially identified, later developed into multiple nodules. The T04 mouse died at 8 weeks, and autopsy showed hepatocellular carcinoma; however, liver cancer had not been confirmed by microCT imaging up to this point. Consequently, the first time-point at which liver cancer was detected by microCT and tissue pathology was 8 weeks. In one mouse (T01), in which contrast agent injection failed, cancer nodules were not confirmed by microCT till 12 weeks; however, liver cancer was confirmed at 12 weeks on pathology. Thus, in the remaining experimental mice (T02, T03, T05, T06) in which liver cancer induction and contrast agent injection were both successful, nodular liver cancer was first identified on microCT images at 8-12 weeks.

Growth of liver cancer and formation of new nodules were identified by microCT imaging, and cancer was confirmed in all animals on histopathology. One and 2 nodules developed in T05 and T06 mice at 10 weeks, respectively, and 7 nodules developed in T02 at 12 weeks. Images of the liver parenchyma in the experimental mice group became quite heterogeneous during the period of 6-8 weeks when compared with images of control group mice at the same time points and previous images of the same mice. At 12 weeks, autopsy was performed on 2 mice (T05 and T06) with confirmed liver cancer by microCT scan, one mouse (T01) in which contrast agent injection failed, and one control group mouse (C02). At 14 weeks, autopsy was performed on the T03 mouse that had

Table 1. Summary of Experimental Results.

Subjects	Time after cancer induction (weeks)						
	2	4	6	8	10	12	14
T03	-	-	-	T(1)	T(5)	T(m)	T(m), A(+)
T05	-	-	-	-	T(1)	T(m), A(+)	
T06	-	-	-	-	T(2)	T(5), A(+)	
T02	-	-	-	-	-	T(7)	T(m), A(+)
T04	-	-	-	-, A(+)			
T01	-	-	-	-	-	-, A(+)	
C02	-	-	-	-	-	-, A(-)	
C01	-	-	-	-	-	-	-, A(-)
N01[1]							-, A(-)

-, Liver cancer(-) on microCT images. A(+): Liver cancer (+) at autopsy, A(-): liver cancer (-) at autopsy. T(number): Number of cancer nodules observed on microCT image. T(m): Multiple ($\geq$10) cancer nodules observed on the microCT images. Injection of contrast media failed in mouse T01, which was scanned for up to 12 weeks and then autopsied. Mouse T04 died at 8 weeks.
[1]For N01, microCT was not performed at 2-12 weeks.

developed earliest liver cancer, the T02 mouse that developed latest liver cancer, one control group mouse (C01), and one normal mouse (N01). A summary of the results is provided in Table 1.

Evaluation of Liver Cancer Formation and Longitudinal Imaging of Cancer Nodules

For the T03 mouse, the cancerous lesion was identified and changes in its size as well as the development of additional nodules were observed until the 14th or last experimental week, demonstrating longitudinal imaging of cancer nodules. In this mouse, a nodule of 0.60 × 0.73 mm had developed at 8 weeks, and it became 1.13 × 1.26 mm by 10 weeks, 1.26 × 1.46 mm by 12 weeks, and 1.59 × 1.66 mm by 14 weeks (Figure 3). There was one nodule at 8 weeks, 5 at 10 weeks, and multiple nodules at 12 weeks. The results of longitudinal imaging in T03 are summarized in Table 2.

Mean and SD of Hepatic Parenchymal Attenuation of the Right Hepatic Lobe ROI in the Normal Mouse (N01)

MicroCT images were taken from a normal mouse (N01) at 14 weeks, to obtain a reference value (Hounsfield Unit; HU) for comparing the mean and SD of hepatic parenchymal attenuation after contrast agent injection. N01 was subsequently sacrificed and autopsied. The mean value and SD of hepatic parenchymal attenuation in the right hepatic lobe ROI of this normal mouse were measured 5 times and averaged to calculate the reference value. The mean (SD) liver parenchymal attenuation values of 5 scans from the N01 mouse were 246 (27.23), 247 (26.81), 249 (27.63), 247 (27.24), and 246 (27.51), respectively. The average mean (SD) liver parenchymal attenuation value was 247 (27.28) HU.
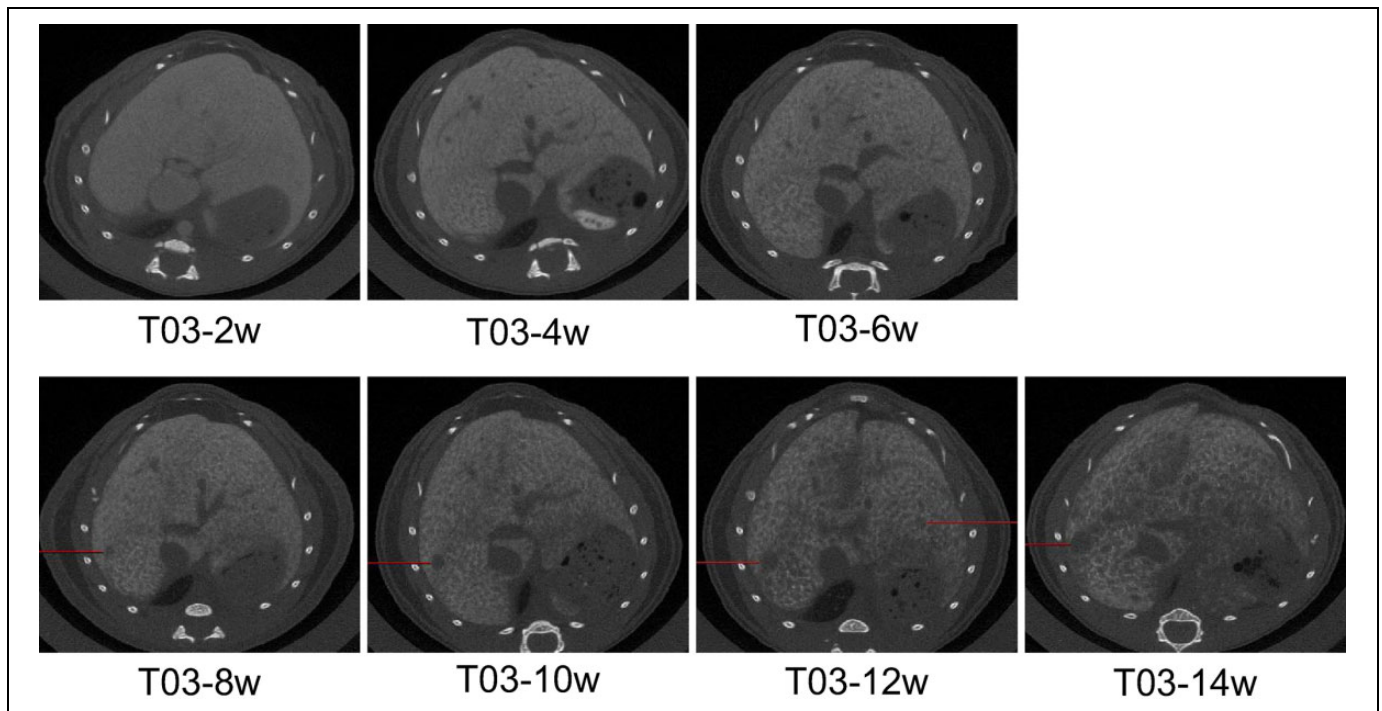
Figure 3. Longitudinal imaging of hepatic nodules in T03 mouse: at 8 weeks, a single nodule developed in mouse T03, and growth of this nodule was monitored over time. Multiple nodules were observed from 12 weeks.

Table 2. The Results for Longitudinal Imaging in T03 Mouse.[a]

Time after cancer induction (weeks)	Number of nodules	Size of target lesion
2		
4		
6		
8	1	0.60×0.73 mm
10	5	1.13×1.26 mm
12	Multiple	1.26×1.46 mm
14	Multiple	1.59×1.66 mm

[a]The target lesion was set as the earliest detected liver cancer nodule, and the size of the target lesion was measured over time.

Mean and Standard Deviation of Hepatic Parenchymal Attenuation in the Right Hepatic Lobe ROIs of Experimental and Control Mice After Contrast Enhancement

The mean value of hepatic parenchymal attenuation in the control and experimental mice remained fairly constant over time. The SD of the degree of attenuation, which reflects the heterogeneous contrast enhancement of the hepatic parenchyma, rose slowly in all mice. The ratio and extent of elevation were greater in the experimental group than in the control group, In the experimental group, the increase was the greatest in the mouse in which liver cancer was induced the earliest (T03). The results are summarized in Table 3 and Figure 4.

Histopathological Results

The histopathological results are shown in Figure 5. In all 6 experimental mice, liver cancer cells were confirmed. A common finding was that nodular hepatic cancer cells of various sizes were distributed throughout the parenchyma, and diffuse hepatocellular carcinoma cells were located between these nodules. In the control group, Kupffer cells were evenly distributed in the parenchyma, and occasional clustering of Kupffer cells (each containing approximately 2 Kupffer cells) were observed. On the other hand, mice in the experimental group had a relatively uneven distribution of Kupffer cells, and the size of individual Kupffer cells was also larger. Additionally, clustered Kupffer cells (each containing 3 to 4 Kupffer cells) were frequently observed around the vessels. Kupffer cells were observed more frequently when the size of liver cancer nodules was small, and more sparsely when nodules were large.

Discussion

The microCT scan images with the normal parenchyma alone enhanced well with contrast agent and were obtained in all 43 scans. Liver cancer induction was successful in all 6 experimental mice. Our results indicate that the approach using the CRISPR/Cas9 technique, nanoparticle contrast agent, hydrodynamic injection, and microCT imaging is an efficient method for generation and long-term imaging of liver cancer in animal models. The mice underwent several stressful events, such as hydrodynamic injections that temporarily but markedly

Table 3. Mean and Standard Deviation of Hepatic Parenchymal Attenuation (HU) and Ratio With Normal Mouse After Contrast Enhancement.[a]

	Mean (SD)							
	C01		C02		T02		T03	
Time after cancer induction (weeks)	HU	Ratio	HU	Ratio	HU	Ratio	HU	Ratio
2	377 (26.18)	1.53 (0.96)	358 (25.18)	1.45 (0.92)	375 (26.21)	1.51 (0.96)	389 (26.95)	1.57 (0.99)
4	402 (31.35)	1.63 (1.15)	359 (29.44)	1.45 (1.08)	391 (34.78)	1.58 (1.27)	412 (39.99)	1.67 (1.47)
6	410 (41.22)	1.66 (1.51)	372 (30.54)	1.51 (1.12)	407 (43.28)	1.65 (1.59)	400 (51.92)	1.62 (1.90)
8	392 (40.92)	1.59 (1.50)	359 (36.99)	1.45 (1.36)	357 (36.91)	1.45 (1.35)	408 (49.05)	1.65 (1.80)
10	409 (41.65)	1.66 (1.53)	343 (36.53)	1.39 (1.34)	367 (43.49)	1.49 (1.59)	390 (55.97)	1.58 (2.05)
12	399 (46.24)	1.62 (1.70)	365 (40.25)	1.48 (1.48)	381 (46.40)	1.54 (1.70)	398 (71.77)	1.61 (2.63)
14	402 (48.08)	1.63 (1.76)	NA	NA	355 (50.55)	1.44 (1.85)	376 (65.10)	1.52 (2.39)

Abbreviations: SD, standard deviation; NA, non-applicable.
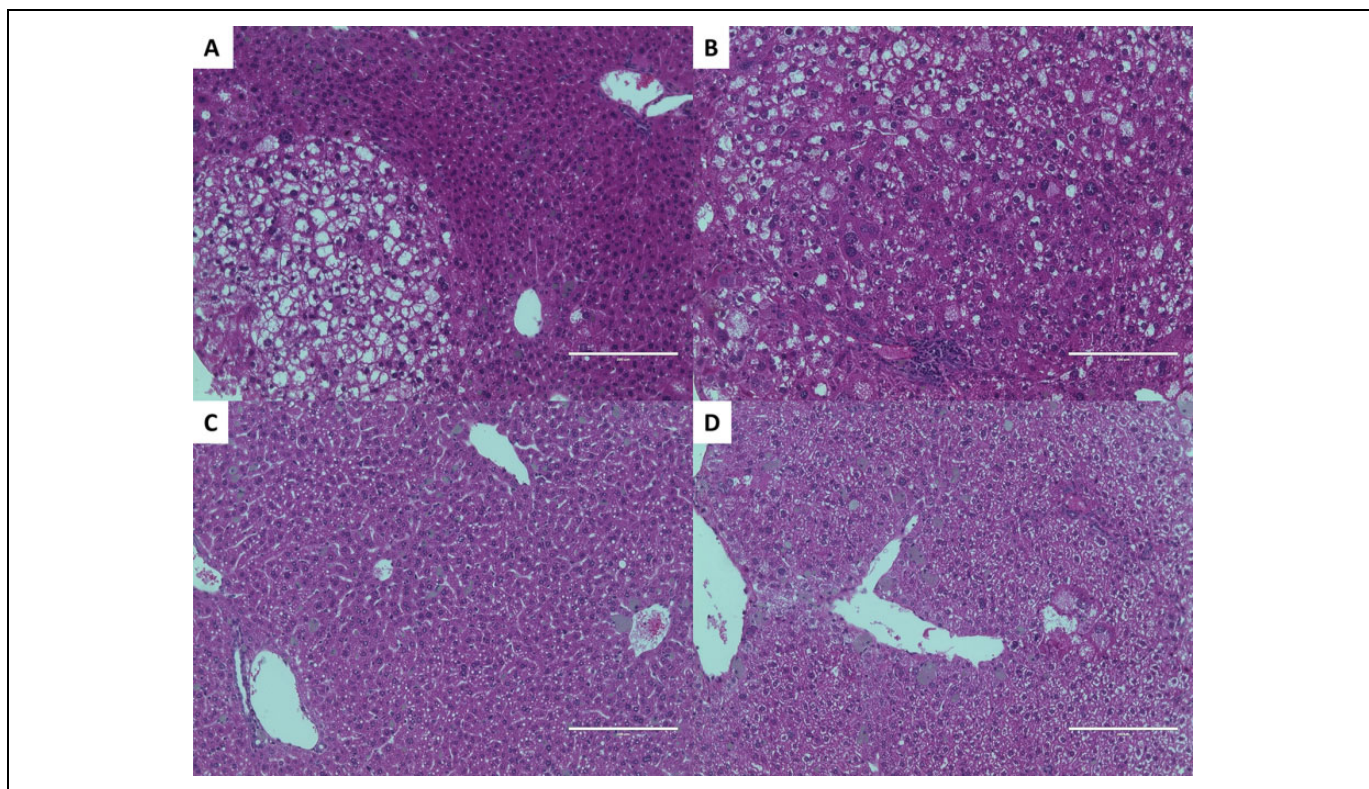[a]C02 mouse was autopsied at 12 weeks.
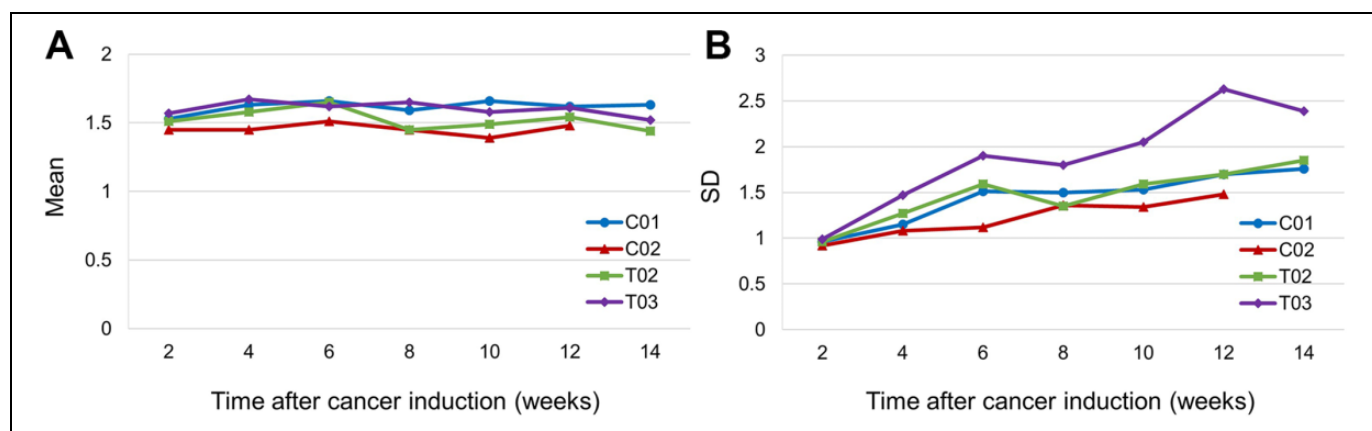
Figure 4. (A) The mean value and (B) the standard deviation of hepatic parenchymal attenuation according to individuals and time-course. A, The mean value of hepatic parenchymal attenuation does not differ significantly according to individuals and time-course. The administered contrast agents are rarely drained out of the liver. B, Standard deviation of attenuation, which reflects heterogeneous contrast enhancement of hepatic parenchyma, increased slowly over time in all mice. The increase was greater in the experimental group than in the control group, particularly in mouse T03, in which liver cancer was detected earliest.

increased blood volumes, CRISPR/Cas9 plasmids that alter the DNA composition of a large number of hepatocytes, injection of nanoparticle contrast agents, and high doses of radiation due to microCT. Nevertheless, the fact that 88% of mice survived without noticeable activity loss suggests that this combined approach is a safe and stable method for producing and studying animal models of liver cancer.

MicroCT using nanoparticle contrast agents has many methodological advantages. With a simple and single administration of contrast agent, a high-resolution image can be obtained quickly, and imaging can be repeated for a long period of time. Anesthesia can be shortened due to the short scan time, thus reducing anesthesia-related risks, such as hypothermia. The microCT device used in this study has an in-built averaging technique, allowing a good quality image to be obtained without complicated procedures, such as tracheal intubation, continuous inhalation anesthesia, or cardiac gating. Fifty microCT scans were successfully performed using the averaging technique and intraperitoneal anesthesia, and none of the images were poor

enough to require retake. Even considering the additional time required for moving the mouse between the cage and CT table and the machine operation time, images could be acquired within a maximum of 5 min per mouse.

The earliest detection of liver cancer using microCT imaging was performed at 8 weeks. The first single nodule was found in mouse T03, and the growth of this nodule was monitored over time. Four weeks after the discovery of the first nodule, nodular liver cancers were clearly distinguished on the images, although diffuse liver cancer could not be clearly observed. On the other hand, histopathological examination revealed a mixture of nodular and diffuse liver cancers. Previous studies that used hydrodynamic injection of liver cancer-inducing agents also found a mixture of nodular and diffuse liver cancer on histopathology; thus, the pattern of formation of hepatocellular carcinoma may be related to the mechanism of the hydrodynamic injection method in which genes flow back to hepatocytes through the hepatic vein.[14,20] With microCT, nodular liver cancer was easy to identify, although the

Figure 5. Histopathological results. A, Nodular liver cancer can be identified in the pathological tissues of mouse T06 autopsied at 12 weeks. B, Diffuse liver cancer can be identified in the pathological tissues of mouse T03 autopsied at 14 weeks. C, Kupffer cells have an even distribution, and sometimes 2 Kupffer cells are clustered around blood vessels, in control mouse C02 autopsied at 12 weeks. D, Kupffer cells are unevenly distributed, with individual Kupffer cells increased in size. In addition, Kupffer cells clustered in groups of 3 to 4 around BLOOD vessels, are often observed in the pathologic tissue of experimental mouse T02 autopsied at 14 weeks.

approach was limited in identifying diffuse liver cancer. Therefore, it is necessary to develop an imaging technique which can accurately reflect the occurrence of diffuse liver cancer.

Contrast agent injection in mouse T01 failed; nevertheless, we continued imaging this mouse for up to 12 weeks; we observed no suspected mass, subtle attenuation differences, or abnormal liver surface nodularity on the microCT image. However, histopathological investigation revealed a large number of liver nodules, illustrating the difficulty of detecting liver cancer without contrast enhancement. On the other hand, in mouse T04, which died at 8 weeks, we were unable to confirm liver cancer by microCT up to the point of death, despite successful contrast enhancement. Multiple liver nodules were detected on histopathology of this mouse, indicating that microCT with contrast agents detect liver cancer later than actual pathological cancerous change.

Heterogeneous enhancement of hepatic parenchyma after contrast agent administration observed in our study has not been reported in previous studies. Although a previous study using the same contrast agent demonstrated that the intensity of contrast enhancement was well maintained for up to 6 months, it did not mention the phenomenon of increasingly heterogeneous enhancement of the liver parenchyma over time.[2] This phenomenon began to appear in the experimental mouse group at around 6 weeks; however, when first discovered, it was not

recognized as a time-dependent change in the distribution of Kupffer cells containing nanoparticle contrast agents. Instead, because these changes were initially only apparent in the experimental mouse group, they were accepted as precursors to liver cancer development. However, we confirmed that the same phenomenon occurred in control mice at 12-14 weeks. Because the phenomenon became more prominent with time, it could be hypothesized that these changes may be the result of changes in the distribution of Kupffer cells in response to nanoparticle contrast agents, and not entirely due to liver cancer. Pathologic examination of experimental and control mice at 12 and 14 weeks revealed Kupffer cells clustering around blood vessels, which was more prominent in experimental mice than in control mice. Moreover, the distribution of Kupffer cells was relatively uneven in the experimental group. Observation of changes in Kupffer cells is necessary for longer periods of time as the findings on histopathological examination at 12 and 14 weeks may change with time and effect the detection of liver cancer. A previous study reported the distribution of Kupffer cells in the liver of 7- to 9-weeks-old rats.[21] Kupffer cells constitute 43% of cells in the periportal area, 28% in the midzonal area, and 29% in the central area, under normal conditions, with the ratio 3:2:2, showing a relatively uniform distribution across the liver. When a foreign material such as latex particle was administered, uptake of the material was observed

in 68% of periportal Kupffer cells and 32% of central Kupffer cells; however, 3 months later, the percentage of periportal Kupffer cells containing foreign materials increased to 75%. In another study of human hepatocellular carcinoma,[22] fewer Kupffer cells were observed in liver cancer tissue than in normal tissue. The larger the liver cancer and lower the grade of cancer differentiation, the fewer Kupffer cells observed. There are also reports of hypertrophy and aggregation of Kupffer cells containing fat vacuoles in perivenular regions in steatohepatitis.[23] From these studies, it can be inferred that the distribution patterns of Kupffer cells in response to foreign materials may have contributed to the distinctive appearance of heterogeneous hepatic parenchymal enhancement over time.

Establishing stable experimental methods which can objectively detect liver cancer nodules and observe changes in their size and number can serve as a powerful tool in many small animal experiments, such as in determining efficiency of new methods of inducing liver cancer. If a specific liver cancer lesion is identified and treated, the change can be assessed over time. In this study, the smallest liver cancer nodule that could be identified on microCT imaging was 0.60 mm, as compared with the minimum discernible size of 0.30 mm in a previous study.[2] Recently, there was a report of an injection of hepatocellular-specific contrast agent (Fenestra LC, MediLumine Inc., Montreal, Canada) into the abdominal cavity to obtain a contrast-enhanced image of the hepatic parenchyma without requiring initial injection through the lateral tail vein[24]; however, serial imaging required multiple injections of contrast media into the abdominal cavity. Furthermore, images need to be obtained 16 h after contrast agent injection to obtain the best image, and the contrast enhancement intensity was lower than that obtained with the ExiTron nano 12000 used in our experiment.[9] In addition to the high success rate of injection through the tail vein, the method introduced in our study is simpler and provides better image quality. In another study using a mouse liver cancer model,[25] liver cancer was induced and nano-emulsion contrast agents containing iodinated oil cores were injected. However, long-term follow-up was not performed, unlike in our study. Considering these previous successful longitudinal imaging studies and the results of our own study,[2,24-26] longitudinal imaging using nanoparticle contrast agents and microCT may offer an effective tool for the follow-up of liver cancer mouse models.

In the mean and SD measurements of hepatic parenchymal attenuation (HU) after contrast enhancement in the right hepatic lobe ROI of control and experimental mice, the mean value remained almost unchanged over time. This suggests that nanoparticle contrast agents captured in Kupffer cells are rarely released from the liver for a long period of time. The slight increase in the standard deviation of this attenuation value in all mice suggests that change in the distribution of Kupffer cells containing nanoparticles is a common phenomenon in both experimental and control groups. In the future, additional experiments will be needed to examine the relationship between the distribution of Kupffer cells and microCT image characteristics.

The significance of this study in terms of causing and identifying liver cancer was to verify the effectiveness of the liver cancer induction method by imaging the liver cancer induced by CRISPR/Cas9 and hydrodynamic injection method on microCT for the first time. In addition, our experimental methodology is expected to be useful as a tool for precise treatment, as it allows for the evaluation of in vivo responses to treatments. An advantage of the nanoparticle contrast agent, such as the ExiTron nano used in this study, is that the contrast enhancement remained stable for a long time, as we confirmed. However, our finding of heterogeneous contrast enhancement of hepatic parenchyma, which can lead to deterioration of image quality and misinterpretation of results, has not been reported previously. We predict that the mechanism may involve changes in the distribution of Kupffer cells. Heterogeneous hepatic parenchymal enhancement may cause errors in the interpretation of images based on nanoparticle contrast agents that act on Kupffer cells; therefore, further studies are needed to ensure accurate recognition and elucidation of the underlying mechanism.

Conclusions

In summary, we present a practical and convenient experimental method for inducing liver cancer and monitoring its development and changes over time. This method may be useful for evaluating the efficiency of different liver cancer induction methods, evaluating the characteristics of induced liver cancer, selecting the appropriate size of liver cancer for assessing treatment efficacy, and confirming the response to treatment.

Abbreviations

C, Control mouse; Cas9, CRISPR-associated protein 9; CRISPR, Clustered Regulatory Interspaced Short Palindrome Repeats; CT, Computed Tomography; Gy, Gray; HU, Hounsfield Unit; H&E, Hematoxylin and Eosin; N, Normal mouse; PTEN, Phosphatase and tensin homolog; ROI, Region of Interest; SD, Standard deviation; T, Experimental mouse.

Authors' Note

The experiment was approved by the Ethics Committee on the Use and Care of Animals of the Dongnam Institute of Radiological and Medical Sciences.

Declaration of Conflicting Interests

The author(s) declared no potential conflicts of interest with respect to the research, authorship, and/or publication of this article.

ORCID iD

Eunji Kim ⓘ https://orcid.org/0000-0002-0565-9301

Supplemental Material

Supplemental material for this article is available online.

References

1. Zucman-Rossi J, Villanueva A, Nault JC, Llovet JM. Genetic landscape and biomarkers of hepatocellular carcinoma. *Gastro-enterology*. 2015;149(5):1226-1229. doi:10.1053/j.gastro.2015. 05.061

2. Liu CN, Morin J, Dokmanovich M, et al. Nanoparticle contrast-enhanced micro-CT: a preclinical tool for the 3D imaging of liver and spleen in longitudinal mouse studies. *J Pharmacol Toxicol Methods*. 2019;96:67-77. doi:10.1016/j.vascn.2019.02.003

3. Ashton JR, West JL, Badea CT. In vivo small animal micro-CT using nanoparticle contrast agents. *Front Pharmacol*. 2015;6:256. doi:10.3389/fphar.2015.00256

4. Hallouard F, Anton N, Choquet P, Constantinesco A, Vandamme T. Iodinated blood pool contrast media for preclinical X-ray imaging applications—a review. *Biomaterials*. 2010;31(24): 6249-6268. doi:10.1016/j.biomaterials.2010.04.066

5. Li X, Anton N, Zuber G, Vandamme T. Contrast agents for pre-clinical targeted X-ray imaging. *Adv Drug Deliv Rev*. 2014;76: 116-133. doi:10.1016/j.addr.2014.07.013

6. Schambach SJ, Bag S, Schilling L, Groden C, Brockmann MA. Application of micro-CT in small animal imaging. *Methods*. 2010;50(1):2-13. doi:10.1016/j.ymeth.2009.08.007

7. Badea CT, Hedlund LW, De Lin M, Mackel JFB, Johnson GA. Tumor imaging in small animals with a combined micro-CT/ micro-DSA system using iodinated conventional and blood pool contrast agents. *Contrast Media Mol Imaging*. 2006;1(4): 153-164. doi:10.1002/cmmi.103

8. Rothe JH, Rudolph I, Rohwer N, et al. Time course of contrast enhancement by micro-CT with dedicated contrast agents in normal mice and mice with hepatocellular carcinoma: comparison of one iodinated and two nanoparticle-based agents. *Acad Radiol*. 2015;22(2):169-178. doi:10.1016/j.acra.2014.07.022

9. Mannheim JG, Schlichthaerle T, Kuebler L, et al. Comparison of small animal CT contrast agents. *Contrast Media Mol Imaging*. 2016;11(4):272-284. doi:10.1002/cmmi.1689

10. Das NM, Hatsell S, Nannuru K, et al. In vivo quantitative micro-computed tomographic analysis of vasculature and organs in a normal and diseased mouse model. *PLoS One*. 2016;11(2): e0150085. doi:10.1371/journal.pone.0150085

11. Xue W, Chen S, Yin H, et al. CRISPR-mediated direct mutation of cancer genes in the mouse liver. *Nature*. 2014;514(7522): 380-384. doi:10.1038/nature13589

12. Li J, Yao Q, Liu D. Hydrodynamic cell delivery for simultaneous establishment of tumor growth in mouse lung, liver and kidney. *Cancer Biol Ther*. 2011;12(8):737-741. doi:10.4161/cbt.12.8.16442

13. Dalsgaard T, Cecchi CR, Askou AL, et al. Improved lentiviral gene delivery to mouse liver by hydrodynamic vector injection through tail vein. *Mol Ther Nucleic Acids*. 2018;12:672-683. doi: 10.1016/j.omtn.2018.07.005

14. Suda T, Liu D. Hydrodynamic gene delivery: its principles and applications. *Mol Ther*. 2007;15(12):2063-2069. doi:10.1038/sj. mt.6300314

15. Kang JH, Mori T, Niidome T, Katayama Y. A syngeneic hepato-cellular carcinoma model rapidly and simply prepared using a hydrodynamics-based procedure. *Vet J*. 2009;181(3):336-339. doi:10.1016/j.tvjl.2008.04.001

16. Yeh MM, Yeung RS, Apisarnthanarax S, et al. Multidisciplinary perspective of hepatocellular carcinoma: a Pacific Northwest experience. *World J Hepatol*. 2015;7(11):1460-1483. doi:10. 4254/wjh.v7.i11.1460

17. Bimonte S, Barbieri A, Palaia R, et al. An overview of loco-regional treatments in patients and mouse models for hepatocel-lular carcinoma. *Infect Agent Cancer*. 2015;10:9. doi:10.1186/ s13027-015-0004-2

18. Moon RT, Kohn AD, De Ferrari GV, Kaykas A. WNT and beta-catenin signalling: diseases and therapies. *Nat Rev Genet*. 2004; 5(9):691-701. doi:10.1038/nrg1427

19. Ally A, Balasundaram M, Carlsen R, et al. Comprehensive and integrative genomic characterization of hepatocellular carcinoma. *Cell*. 2017;169(7):1327-1341.e23. doi:10.1016/j.cell.2017.05.046

20. Liu YT, Tseng TC, Soong RS, et al. A novel spontaneous hepa-tocellular carcinoma mouse model for studying T-cell exhaustion in the tumor microenvironment. *J Immunother Cancer*. 2018;6(1): 144. doi:10.1186/s40425-018-0462-3

21. Bouwens L, Baekeland M, De Zanger R, et al. Quantitation, tissue distribution and proliferation kinetics of Kupffer cells in normal rat liver. *Hepatology*.1986;6(4):718-722. doi:10.1002/hep. 1840060430

22. Liu K, He X, Lei XZ, et al. Pathomorphological study on location and distribution of Kupffer cells in hepatocellular carcinoma. *World J Gastroenterol*. 2003;9(9):1946-1949. doi:10.3748/wjg. v9.i9.1946

23. Lefkowitch JH, Haythe JH, Regent N. Kupffer cell aggregation and perivenular distribution in steatohepatitis. *Mod Pathol*. 2002; 15(7):699-704. doi:10.1097/01.MP.0000019579.30842.96

24. Sweeney N, Marchant S, Martinez JD. Intraperitoneal injections as an alternative method for micro-CT contrast enhanced detec-tion of murine liver tumors. *Biotechniques*. 2019;66(5):214-217. doi:10.2144/btn-2018-0162

25. Anton N, Parlog A, Bou About G, et al. Non-invasive quantitative imaging of hepatocellular carcinoma growth in mice by micro-CT using liver-targeted iodinated nano-emulsions. *Sci Rep*. 2017; 7(1):13935. doi:10.1038/s41598-017-14270-7

26. Keshavarzi M, Sorayayi S, Jafar Rezaei M, et al. MicroRNAs-based imaging techniques in cancer diagnosis and therapy. *J Cell Biochem*. 2017;118(12):4121-4128. doi:10.1002/jcb.26012